River Flow 2010 - Dittrich, Koll, Aberle & Geisenhainer (eds) - © 2010 Bundesanstalt für Wasserbau ISBN 978-3-939230-00-7

Numerical simulation of spheres moving and colliding close to bed streams, with a complete characterization of turbulence

Fabián A. Bombardelli, Andrea E. González & Patricio A. Moreno[1]
Department of Civil and Environmental Engineering, University of California, Davis, United States of America. [1]*Also, Escuela de Ingenieria en Obras Civiles, Universidad Diego Portales, Santiago, Chile.*

Víctor M. Calo
Applied Mathematics and Computational Sciences and Earth Science and Engineering, King Abdullah University of Science and Technology (KAUST), Kingdom of Saudi Arabia.

ABSTRACT: This paper presents some results regarding the motion of solid particles as bed-load in streams, in the range of sands. In order to effectively simulate this important problem avoiding excessive computational costs, we followed a decoupled approach, which uses a computed turbulent velocity field for a smooth flat plate as a surrogate of the three-dimensional (3D) turbulent conditions close to the bed in streams. Because these two flows are not the same, we first tested that the basic turbulence statistics for this velocity field did not differ significantly from those in an open-channel flow. We then tracked particles with a 3D Lagrangian model. The Lagrangian model also includes the calculation of the particle rotation and a generalized algorithm for particle collisions with walls and with other particles. Numerical simulations of several particle sizes were performed and the results were compared with previous experimental data, with good agreement.

Keywords: Saltation; Bed-load transport; Turbulent velocity field; 3D Lagrangian model; Flow in a flat plate; Turbulence statistics; Particle rotation; Inter-particle collisions.

1 INTRODUCTION

The motion of solid particles as bed-load in streams has attracted an important level of attention recently. To date, most numerical simulations use the semi-logarithmic velocity distribution to represent the velocity field which particles are subjected to. Although this velocity distribution is a very good approximation of the average flow conditions in boundary layers, it obviously does not account for the time dependence of turbulence. In order to potentially improve predictions of bed-load transport and gain more insight into the physics of the problem it is necessary to provide a more realistic velocity field capable of reproducing the turbulent characteristics of natural flows.

The ideal situation would be to perform Direct Numerical Simulations (DNS) and to compute the motion of multiple particles, accounting for the volume occupied by them. Unfortunately, such a paradigm is currently out of the picture, given the enormous computational time associated with solving the velocity field surrounding each particle. In some approaches, researchers have solved for the motion of groups of particles in an aggregated manner.

In this paper, we follow an intermediate step, which uses a computed turbulent velocity field for a smooth flat plate to act as a surrogate of the three-dimensional (3D) turbulent conditions close to the bed in streams. Although the two flows are different, insight can be gained with these computations. The results of a high-resolution 3D turbulent velocity field developed by Calo (2004) are coupled with a 3D particle tracking Lagrangian model (González, 2008). By using this velocity field, the effect of turbulence on the particle motion close to the bed is studied, assuming a one-way coupling between the moving particles and the flow field. Future analyses will include rough boundaries.

2 DESCRIPTION OF THE NUMERICAL SIMULATION OF THE FLOW FIELD

2.1 *HR3D simulation description and analysis*

A highly-resolved three-dimensional (called herein HR3D) flow velocity field obtained by Calo (2004) reproduces the ERCOFTAC T3A test case

(Roach & Brierley, 1992), which involves a bypass transition to turbulence on a flat plate due to free-stream turbulence passing above the plate. The velocity field used in this work considers only a sub-section of the simulation, where the turbulence has already developed for some important distance.

In the HR3D flow simulation all lengths are made non-dimensional using the boundary layer thickness δ_0 at the inlet of the domain. The domain box is 620 δ_0, 40 δ_0 and 30 δ_0 in the longitudinal, vertical and transverse directions, respectively. The velocity scale selected was U_m, which represents the unperturbed stream-wise velocity of the fluid far away from the wall.

The HR3D flow velocity field was obtained through a second order, finite-volume code developed by Pierce & Moin (2001) and Jacobs & Durbin (2001) at the Center for Turbulence Research, Stanford University. In the code, the Navier-Stokes equations are solved on a staggered grid. All fluxes in the wall-normal direction are integrated implicitly using a Crank-Nicolson scheme (convective terms are linearized). The pressure is integrated fully implicitly. No closure for turbulence was used, which could yield to Direct Numerical Simulation (DNS) with appropriate spatial mesh sizes. (For the spatial steps used in Calo's simulation, the HR3D result is *close* to a DNS but it cannot be rigorously considered DNS.)

The HR3D simulation used in this paper considers a value of the Reynolds number, defined as $\mathrm{Re}_\delta = U_m \delta_0 / \nu$, equal to 795. Given the inherent differences between the boundary layer in a flat plate and in an open-channel flow, it is necessary to discuss the meaning of the coupling of the particle tracking code with the HR3D turbulent velocity field, a task done below.

2.2 *Boundary-layer flows in a flat plate and in channels*

It is accepted that a high degree of similarity exists between boundary-layer flows over flat plates and channel flows, in particular open-channel flows, which are the interest of this work (see Gad-El-Hak, 2000; Davidson, 2005). Obviously, the most important difference lies on the spatially developing character of the former. In order to assess the feasibility of using Calo's velocity field as a surrogate of the velocity field in an open channel, the features of both types of flow are discussed in this section.

A short, but very useful analysis of similarities and differences between turbulent boundary-layer, flat-plate flows, and channel flows is presented by Nieuwstadt & Bradshaw (1997) and Ashrafian (2004). The main differences could be summarized as follows: 1) The turbulent/ambient flow interface is absent in channel flows; 2) the free surface (present only in open-channel flows) suppresses the vertical movement of eddies, as opposed to the outer layer of a flat-plate flow (Nezu & Nakagawa, 1993); 3) in channel flows, the excessive energy is transported by turbulent diffusion to the free-surface region where it compensates the dissipation (Nezu & Nakagawa, 1993), whereas in boundary-layer flows, the extra energy is used to sustain the thickening of the layer (Jiménez, 2004); and 4) the wake strength for channel flows is much smaller than the counterpart in boundary-layer flows (Johnson, 1998).

Despite all these differences between boundary-layer flows over a flat plate and in open channels, the logarithmic profile which describes the mean stream-wise velocity close to the wall has been found to be applicable to all wall-bounded flows (Gad-El-Hak, 2000). In this regard, Wei et al. (2005) present "compelling evidence" of the logarithmic character of the mean profile in a large section of both channel and boundary-layer, flat-plate flows. Further, the structure of the turbulence can be expected to be similar in both cases, close enough to the wall. Davidson (2005, page 137) emphasizes that "there is a region near the wall where the flow does not know or care about the gross details of the outer flow." Therefore, the turbulent velocity field HR3D is capable of approximating both the mean velocity and turbulence statistics of an open-channel flow. Further, since the interest of the saltating motion is on the region close to the bed (z/depth<0.05) the use of the HR3D velocity field yields accurate results.

In order to corroborate that the turbulence parameters defined for an open-channel flow are well reproduced in the HR3D, it is necessary first to analyze both flows through a dynamic similarity analysis.

2.3 *Dynamic similarity*

When both viscous and gravitational effects are important, the Froude and Reynolds numbers, Fr and Re, respectively, have to be equal to achieve dynamic similarity between two flows. For a flow past an object in a fluid (such as particles saltating at the bottom of a channel), gravity is only important if surface waves are generated (Kundu & Cohen, 2008). (It is assumed herein that the water density is quasi-uniform close to the bed to avoid the need for consideration of differences in density -via the densimetric Froude number- as a source of currents.) In boundary-layer flows, the Reynolds number is the only dimensionless number that needs to be equal in the two flows. Thus, the HR3D velocity field represents accurately the

flow field interacting with salting particles, provided that the same Reynolds number is preserved.

This similitude has been used before in several opportunities. Rouse et al. (1958) employed this procedure to study hydraulic jumps in water by using wind-tunnel results (see discussion in González, 2008).

2.4 *Simulated flow characteristics*

Time-averaged velocities obtained from the HR3D simulation should be close to well known expressions for the mean flow velocity in a turbulent open channel (i.e., the law of the wall). To check this, it is necessary to relate the velocity and time scales used in the HR3D simulation with those of the problem. The HR3D flow simulation includes U_m and δ_0 as velocity and length scales, while the particle model (to be described below) has the wall-friction (shear) velocity (u_*) and the particle diameter (d_p) as scales. Using the time-averaged values of the simulated velocity field (expressed in dimensionless terms as u^f/U_m), a relationship between velocity scales is found:

$$\frac{u^f}{U_m} = \frac{u^f}{u_*}\frac{u_*}{U_m} \tag{1}$$

From Eq. (1), u_f/u_* can be obtained for comparison with the semi-logarithmic velocity law. Defining $A = u_*/U_m$, the length scales can be in turn related as follows:

$$\frac{z\,u_*}{\nu} = z^+ = \frac{z}{\delta_0}\mathrm{Re}_\delta\, A \tag{2}$$

where the location of the nodes in the HR3D simulations are expressed in terms of z/δ_0. Using Eqs. (1) and (2), the values u^f/U_m, z/δ_0 and Re_δ from the HR3D velocity field are converted to values of u^f/u_* and z^+ for comparison with the log-law of the wall. The value of A was determined by trial and error, adopting the value that produces the best fit between the HR3D numerical results and the semi-logarithmic expression for the velocity profile in the case of a smooth channel. The value of A was determined to be equal to 0.045, as shown in Figure 1.

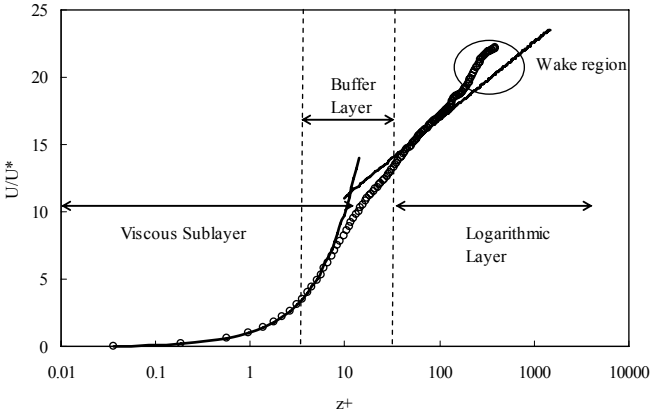

Figure 1: Comparison between the mean stream-wise fluid velocity obtained from the HR3D simulation and the semi-logarithmic expression for the velocity profile in a smooth turbulent open-channel flow. Solid lines represent that expression, and circles represent data obtained from numerical simulation. The numerical results follow the law of the wall.

Since the Reynolds number must be preserved between the open-channel flow and the HR3D flow, another relationship between non-dimensional numbers can be predicated:

$$\mathrm{Re}_\delta = \frac{U_m\delta_0}{\nu} = \frac{U_m}{u_*}\frac{\delta_0}{d_p}\frac{u_* d_p}{\nu} = R_p\sqrt{\tau_*}\,\frac{1}{A}\frac{\delta_0}{d_p} \tag{3}$$

where R_p = explicit particle Reynolds number, equal to $(R\,g\,d_p^3)^{0.5}/\nu$, ν = kinematic viscosity of water, $R = (\rho_s/\rho - 1)$, with ρ and ρ_s indicating the water and sediment densities, respectively; and $\tau_* = u_*^2/(g\,R\,d_p)$, where g = acceleration of gravity. It becomes clear from Eq. (3) that δ_0/d_p can be obtained for a given particle size and flow condition (u_*).

Nezu & Nakagawa (1993) presented the results of extensive experimental research in turbulent open-channel flows. They obtained universal expressions for turbulence intensities (denoted by u_f', v_f' and w_f', which represent the stream-wise, span-wise and wall-normal components of the fluid turbulence intensity, respectively), and turbulent kinetic energy (TKE_f), normalized with the friction velocity and the friction velocity squared, respectively.

In the case of a boundary-layer flow over a flat plate, there is no clear definition for H_c. In order to compare the numerical results of turbulence intensities and turbulent kinetic energy between the flat-plate and boundary-layer flows, H_c was assumed to be equal to the depth of the simulation space. Distributions for the flow turbulence intensity of the flow in each direction and for the turbulent kinetic energy (TKE_f) computed from the HR3D simulation were compared with the experimental regressions developed by Nezu & Nakagawa Figure 2 shows, for instance, the stream-wise component of the velocity. In general, good

agreement was observed between the different vertical profiles obtained from the numerical simulation and the empirical expressions.

Results from the HR3D simulation present the expected exponential decrease with the distance from the wall, in all four variables.

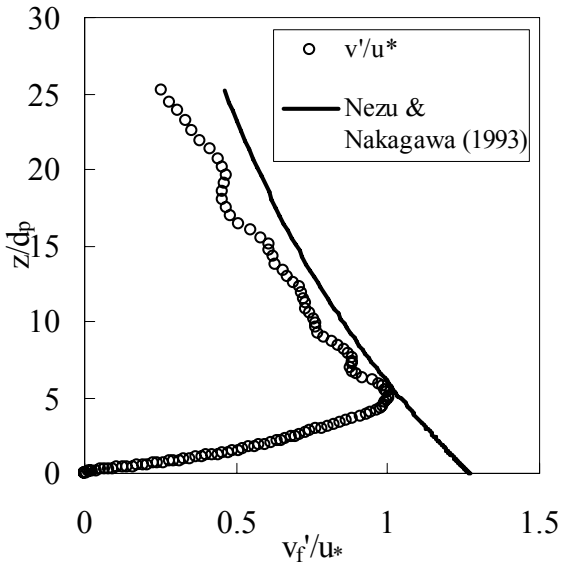

Figure 2: Turbulence intensities from the numerical simulation (circles) compared with the experimental regression suggested by Nezu & Nakagawa (1993) (solid line). Spanwise component. The same level of agreement was found for other components and for the TKE.

Finally, it is necessary to corroborate that the wave-number spectrum obtained from the simulation follows the -5/3 Kolmogorov law in the inertial sub-range, which has been shown to provide important insight into pipe and other shear flows (Gioia & Chakraborty, 2006). The comparison showed that for every velocity component this spectrum model is followed. Figure 3 shows the spectrum of the stream-wise velocity component.

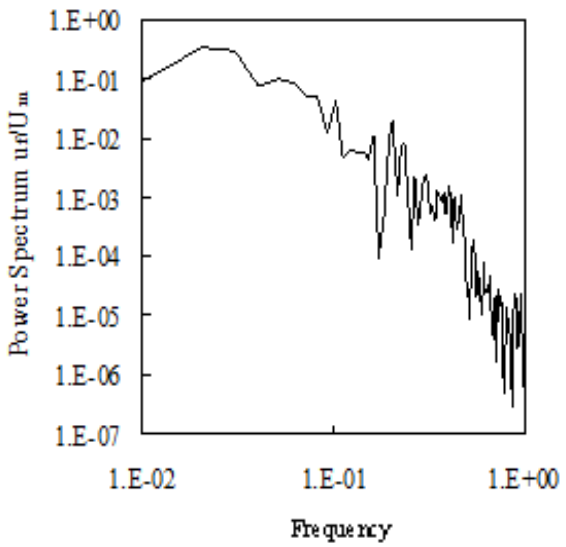

Figure 3: Wave-number spectrum of the velocity component in the stream-wise direction.

It is concluded that the HR3D velocity field represents satisfactorily the turbulent flow in an open channel, both in time-averaged values and turbulence statistics. Thus, the HR3D field was used to track particles moving close to the bed. It was assumed that the effect of the particle volume on the surrounding fluid can be disregarded in first approximation, as done in current approaches.

3 MODEL FOR PARTICLE TRACKING IN A TURBULENT FIELD

3.1 *Equations for particle "flight"*

A 3D particle tracking model was coupled with the data provided by the HR3D velocity field. For this case, the motion of the particles was computed using Eq. (4) below, where the expression for the forces considered the fluctuating and non-uniform nature of the 3D velocity field.

$$\frac{1}{\alpha}\frac{d\vec{u_p}}{dt} = R\frac{d_p\vec{g}}{u_*^2} - \frac{3}{4}C_D\left(\vec{u_p}-\vec{u_f}\right)\left|\vec{u_p}-\vec{u_f}\right| + \frac{9}{\tau_*^{0.25}\sqrt{R_p\pi}}\int_0^t \frac{d}{d\tau}\left(\vec{u_f}-\vec{u_p}\right)\frac{d\tau}{\sqrt{t-\tau}} + C_m\frac{d\vec{u_f}}{dt} + \frac{D\vec{u_f}}{Dt} + \frac{3}{4}\left(\frac{1}{2}\vec{\omega_f}-\vec{\omega}\right)x\left(\vec{u_f}-\vec{u_p}\right) + \frac{3}{4}C_L\left(\left|\vec{u_r}\right|_T^2 - \left|\vec{u_r}\right|_B^2\right)\vec{e} \quad (4)$$

where C_D = drag coefficient, C_L = lift coefficient, u_{rT} = relative velocity vector at the top of the particle, u_{rB} = relative velocity vector at the bottom of the particle, and u_f = fluid velocity; $\alpha = \left(1+R+C_m\right)^{-1}$, where C_m = virtual mass coefficient; t = time coordinate, τ = dummy variable for integration, $\vec{\omega_f}$ is the dimensionless fluid vorticity vector and $\vec{\omega}$ is the non dimensional particle rotation vector. The terms on the right hand side of Eq. (4) consider buoyancy, non-linear drag, the Basset force, the remainder of the virtual mass, fluid acceleration, the Magnus force, and the lift. The operator $d(\cdot)/dt$ indicates the material derivative using the particle velocity and $D(\cdot)/Dt$ uses the fluid velocity.

The model was developed in FORTRAN and can track numerous particles simultaneously, including inter-particle collisions. Details on the model for inter-particle collisions can be found in González (2008).

It is worth noting that the model does not include any stochastic component to enhance the turbulence and uses the resolved velocity field as it was computed.

3.2 *Treatment of the Basset force*

A novel technique is employed in the model to treat the Basset force, as discussed in González et al. (2006), González (2008) and Bombardelli et al. (2008). The technique uses fractional mathematics to approximate the integral of the Basset force and the concept of "memory time period", in order to reduce its computational time and the requirements of storage of the derivatives of velocity in time.

3.3 *Equations for particle rebound with walls*

A stochastic model was employed to analyze the particle rebound with walls, based on modifications of models proposed by Niño & García (1994) and Tsuji et al. (1985). This model assumes that the bed is formed by packed, unimodal spheres, and that the moving particle can hit the particles in the bed with random angles distributed uniformly in a range. Thus, the model computes the velocity in the three directions and the particle rotation after the rebound. The model considers that the diameter of the particles in the bed ($d_{p\,bed}$) is 0.3 mm to maintain the smooth characteristic of the bed, and to have consistency with the velocity field adopted. Using geometrical properties between the moving particle and the particles composing the bed, θ_{crit}, the maximum angle at which the moving particle can hit the bed, was expressed in terms of the particle size at the bed and the incoming particle diameter, where different particle sizes are defined for the bed and the particles in motion. More details can be found in González (2008), Bombardelli et al. (2008) and Bombardelli et al. (2010).

4 MODEL VALIDATION

4.1 *Validation of the model for a single particle*

Simulations corresponding to the experimental conditions presented by Niño & Garcia (1998a, b) were performed for validation purposes. The numerical model was run for a simulation time long enough to have meaningful statistics. In order to remove the effect of the initial conditions, the first jumps were not considered in the statistical analysis.

Figure 4 presents the numerical results obtained for moving particles of R_p = 73 which are compared to experimental results in the range of R_p = 60-90 presented by Niño & García (1998a, b). The figures depict the comparison of the dimensionless particle jump length and the mean stream-wise velocity, with the experimental data, for increasing bottom shear stresses. Both plots include two standard deviations of the mean value. Good agreement was found between the numerical simulation and the experimental data, especially for the jump length. The image of the mean stream-wise velocity shows that the *observed* data do not vary significantly, a feature that somehow defies intuition. The numerical result, on the other hand, shows an increase of that variable with the increase in the value of the shear stress.

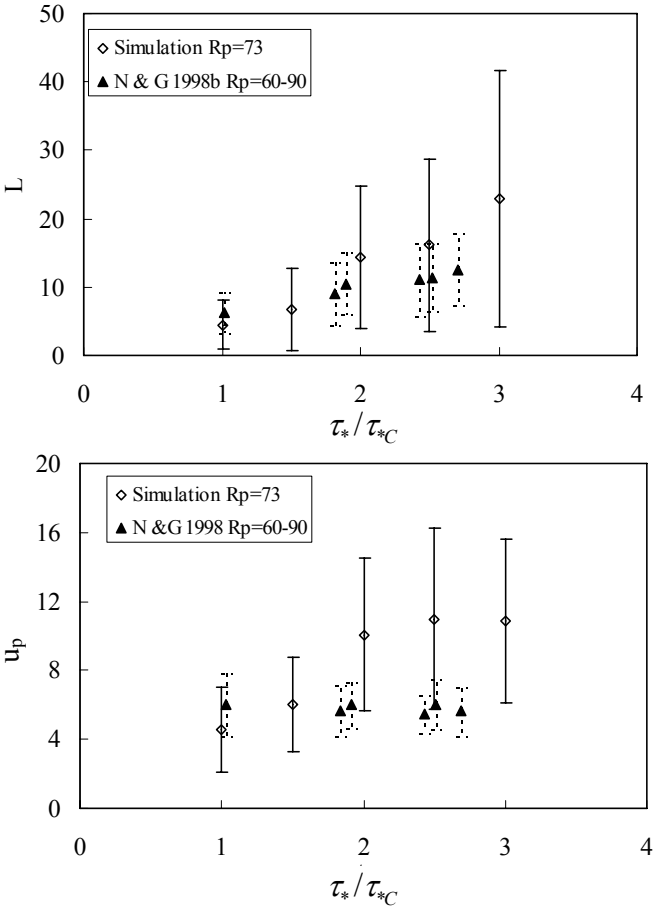

Figure 4: Comparison of simulations with experimental data for the case of a particle moving in a flume and rebounding with the wall. The top figure shows results associated with the particle jump length, and the bottom figure shows the stream-wise mean velocity.

Similar results were obtained for the jump height and the mean particle spinning rate (not shown herein; see González, 2008). We noticed that if the particle velocity is tracked with just an average velocity profile, the ranges of variation of the variables are smaller, due to the fluctuations of velocity of the HR3D velocity field. We also noticed that the agreement with data obtained from the use of the HR3D field slightly improves for some particle sizes, being in general similar to that obtained with the time-averaged velocity profile. More research is thus needed to address this issue further.

4.2 *Model validation for numerous particles*

Simulations were undertaken with the model mimicking the case of multiple particles moving in the same velocity field discussed above.

Figure 5 presents similar plots to those of Figure 4, pertaining to the case of multiple particles moving and colliding in the velocity field, and for two particle sizes: $R_p = 80$ and $R_p = 120$. An acceptable agreement is noticed between simulations and data.

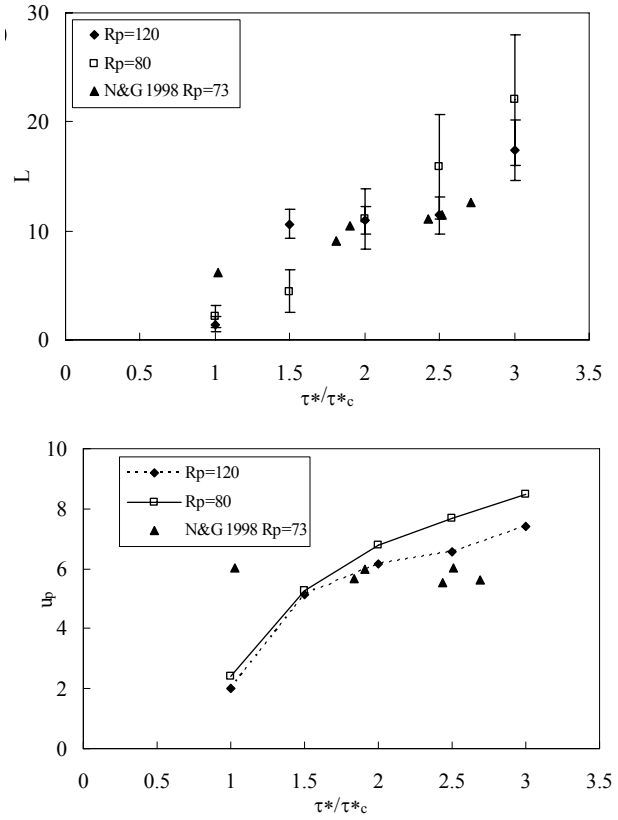

Figure 5: Comparison of simulations with experimental data for the case of multiple particles moving in a flume and rebounding with the wall and colliding among themselves. The top figure shows results associated with the particle jump length, and the bottom figure shows the stream-wise mean velocity.

Further validation of the model was obtained via comparison of both detailed and integrated variables associated with the particle jumps. Take-off angles of the particles after collision, lateral dispersion angle, and the cumulative probability distribution of the absolute value of the deviation angle all show acceptable agreement with data. Figure 6 presents in particular the result regarding the take-off angles of particles.

Figure 7, in turn, compares bed-load transport rates derived from the simulation with multiple particles with well-known expressions. The numerical transport rate can be obtained by just counting the number of particles which cross a specific location of the computational domain in a given period, and multiplying this result by the particle volume. The dimensionless volumetric bed load rate q^* is then calculated as:

$$q^* = \frac{q}{\sqrt{g\,R\,d_p^3}} \tag{6}$$

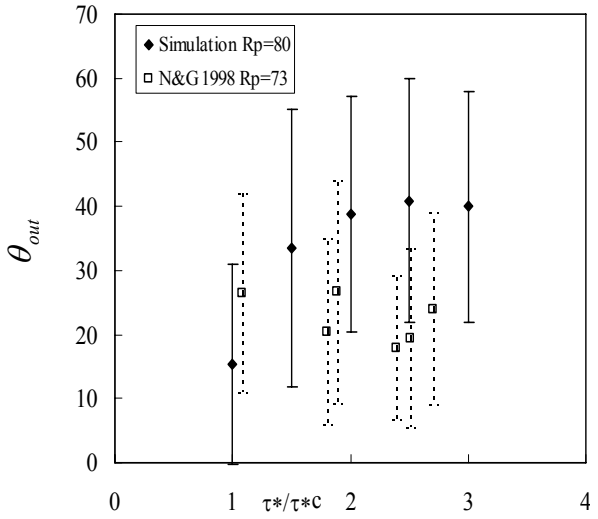

Figure 6: Comparison of simulations with experimental data for the case of multiple particles moving in a flume, rebounding with the wall and colliding among themselves. The figure shows results associated with the take-off angle after collision (θ_{out}). Symbols represent mean values and vertical lines indicate two corresponding standard deviations. $R_p = 80$.

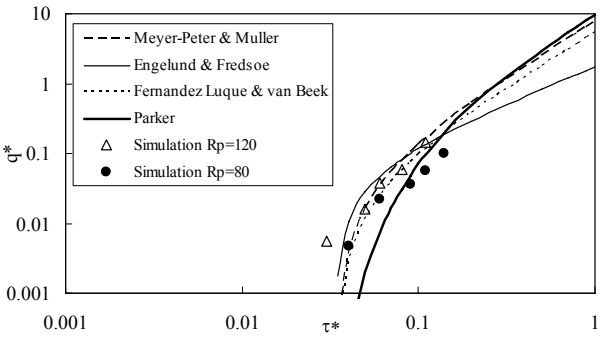

Figure 7: Comparison of numerical results with expressions for bed-load transport rates for the case of multiple particles moving in a flume and rebounding with the wall and colliding among themselves.

Taking into account the uncertainties in the experimental results of bed-load transport, reasonable agreement between model results and expressions by Meyer-Peter-Muller, Fernandez Luque & van Beek, Engelund & Hansen, and Parker, is found.

5 PARTICLE VELOCITY AND TRAJECTORIES

One of the immediate results of the application of the model is that the velocity of the particle following the turbulent field can be obtained. This is shown in Figure 8, where the stream-wise velocity component is shown. It is important to notice the random character of the results. The importance of this result lies in that the particle turbulent kinetic energy and other turbulence statistics can be defined, as done by González (2008).

Figure 9 shows in addition 3D trajectories of multiple particles indicating that the 3D wall-collision algorithm performs adequately.

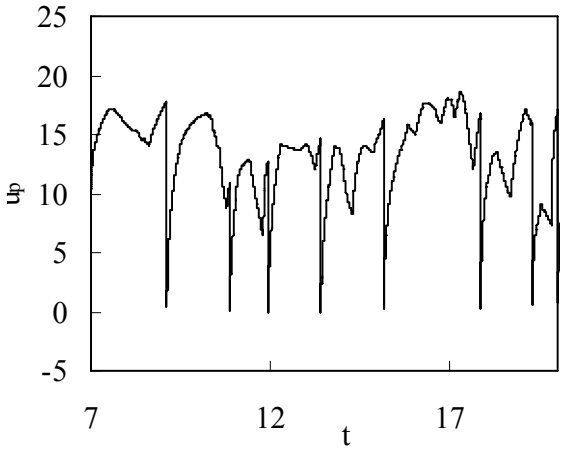

Figure 8: Numerical results regarding the velocity of a particle moving close to a wall in the HR3D velocity field. The result corresponds to the stream-wise velocity component.

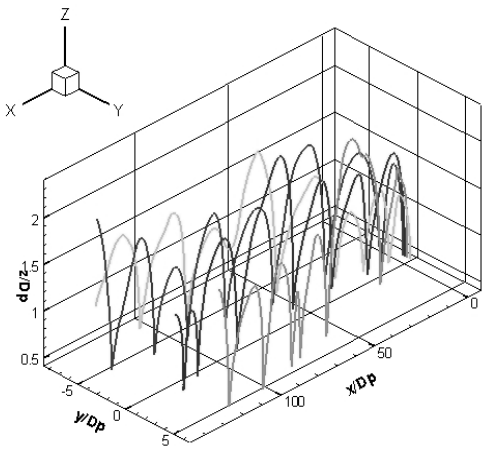

Figure 9: Trajectories of particles from the 3D simulation of saltation of multiple particles.

6 CONCLUSIONS

A comprehensive model for the analysis of the saltating motion of particles has been presented. The model exploits a three-dimensional velocity field past a flat plate in the turbulent portion, and tracks particles with a Lagrangian model in that field. The Lagrangian model includes diverse sub-models for particle rotation, inter-particle collision and a stochastic sub-model for particle collision with solid boundaries.

The results were validated with experimental data obtaining good agreement with them. Once validated, the model was used to compute parameters of interest and to gain insight into the interaction of particles and flow.

REFERENCES

Ashrafian, A. 2004. Numerical investigation of turbulent flow in a channel with rough walls. PhD Thesis. Norwegian University of Science and Technology. Trondheim, Norway.

Bombardelli, F.A., González, A.E. & Niño, Y.I. 2008. Computation of the particle Basset force with a fraccional-derivative approach. Journal of Hydraulic Engineering ASCE. 134 (10), 1513-1520.

Bombardelli, F.A., González, A.E., Moreno, P.A. & Moniz, R. 2010. Generalized algorithms for particle motion and collision with stream beds. Paper in preparation.

Calo, V.M. 2004. Residual-based multiscale turbulence modeling: finite volume simulations of bypass transition. PhD. Dissertation. Stanford University.

Davidson, P.A. 2005. Turbulence: An introduction for scientists and engineers. Oxford University Press.

Gad-El-Hak, M. 2000. Flow Control. Cambridge University Press.

Gioia, G. & Chakraborty, P. 2006. Turbulent friction in rough pipes and the energy spectrum of the phenomenological theory. Phys. Rev. Lett. 96. 4. 044502.

González, A.E., Bombardelli, F.A. & Niño, Y.I. 2006. Towards a direct numerical simulation (DNS) of particle motion near the bed. In: Proceedings of River Flow 2006, Lisbon, Portugal, pp. 799-806.

González, A.E. 2008. Numerical modeling of sediment transport near the bed using a two-phase flow approach. Ph.D. Thesis, University of California, Davis. 188 p.

Jacobs, R. & Durbin, P. 2001. Simulation of bypass transition. J. Fluid Mech. 428. 185-212.

Jiménez, J. 2004. Turbulent flows over rough walls. Annual Rev. of Fluid Mech. 36. 173–196.

Johnson, R.W. 1998. The handbook of fluid dynamics. Boca Raton FA. CRC Press.

Kundu, P.K. & Cohen, I.M. 2008. Fluid Mechanics. Elsevier Academic Press.

Lee, H.Y. & Hsu, I.S. 1994. Investigation of saltating particle motions. ASCE J. of Hyd. Eng.120 (7). 831-845.

Nezu, I. & Nakagawa, H. 1993. Turbulence in Open-Channel Flows. IAHR Monograph Series. Rotterdam. A. A. Balkema.

Nieuwstadt, F.T.M. & Bradshaw, P. 1997. Similarities and differences of turbulent boundary-layer, pipe and channel flow. In Boundary -Layer separation in aircraft aerodynamics. Ed. by Henkes, R.A.W.M., Bakker, P.G. Delft University Press.

Niño, Y. & García, M.H. 1994. Gravel Saltation. 2. Modeling. Water Resources Research 30 (6), 1915-1924.

Niño, Y. & García, M.H. 1998a. Experiments on saltation of sand in water. ASCE J. Hyd. Eng. 124. 1014-1025.

Niño, Y. & García, M.H. 1998b. Using Lagrangian particle saltation observations for beadload sediment transport modeling. Hydrological Processes. 12. 1197-1218.

Pierce, C. & Moin, P. 2001. Progress-variable approach for large eddy simulation of turbulent combustion. Technic-

al Report TF-80, Flow Physics and Computation Division, Department of Mechanical Engineering, Stanford University. Available at http://ctr.stanford.edu/Pierce/thesis.pdf

Roach, P.E. & Brierley, D.H. 1992. The influence of a turbulent free-stream on a zero pressure gradient transitional boundary layer development. Part 1: Test case T3A and T3B. In Numerical Simulation of Unsteady Flows and Transition to Turbulence, ERCOFTAC. Pironneau, O., Rodi, W., Rhyming, I.L., Savill, A.M,Truong, T.V. editors, Cambridge University Press. 319-347.

Rouse, H., Siao, T.T. & Nagaratnam, S. 1958. Turbulence characteristics of the hydraulic jump. Journal of the Hyd. Div. ASCE. Proc. Paper 1528.1-30.

Tsuji, Y., Oshima, T. & Morikawa, Y. 1985. Numerical simulation of pneumatic conveying in a horizontal pipe. KONA 3, 38-51.

Wei, T., Fife, P., Klewicki, J. & McMurtry, P. 2005. Properties of the mean momentum balance in turbulent boundary layer, pipe and channel flows. J. of Fluid Mech. 552. 303-327.